15th Australasian Fluid Mechanics Conference
The University of Sydney, Sydney, Australia
13-17 December 2004

Flows Within a Cylindrical Cell Culture Bioreactor with a Free-Surface and a Rotating Base

J. Dusting, J. Sheridan and K. Hourigan

Fluids Laboratory for Aeronautical and Industrial Research (FLAIR), Department of Mechanical Engineering
Monash University, Victoria, 3800 AUSTRALIA

Abstract

Experimental studies have been conducted in order to identify and investigate flows that are potentially more suited to culturing cells than those commonly found in bioreactors. The tested model has a cylindrical working section with a free surface and a rotating base. Flow visualisation confirms the presence of vortex breakdown bubbles at $Re \geq 780$ for an aspect ratio of 1.5. The central bioreactor region has been characterised using Particle Image Velocimetry and Stereoscopic Particle Image Velocimetry. Shear stress, an important parameter for cell culture applications, has been plotted at various Reynolds numbers, showing a pattern related to the geometry of the vortex breakdown bubble.

Introduction

Strong recent advancements in tissue engineering and cell-based therapeutic research have driven a push to find alternative methods of culturing cells, with the aim to increase the efficiency and productivity of the process. Lately, the development of various perfused vessel and rotational bioreactors has received interest, with some promising results [1, 4]. Progress is still to be made, however, in controlling the fluid dynamic conditions within mixed flask bioreactors. Depending on the cell phenotype, hydrodynamic forces may provide an important stimulatory effect on cell aggregation processes, however excessive shear will impede cell proliferation. Ideally, the bioreactor flow conditions would suit these and other factors such as mixing.

A simplified experimental model has been developed to enhance flow control. The model has a flat bottom disk capable of producing swirling flows far steadier than those produced by standard bioreactor impellers and magnetic stirrers [7]. The working section consists of a cylindrical volume of media devoid of protruding objects that might disturb the flow. A free surface rather than a closed lid is used so as to provide greater aeration while minimising the extent of high-shear boundary regions. This model is suited to the application because it has the potential to produce flows that contain appropriate shear levels, can be adequately mixed and can be characterised experimentally. Detailed studies of flows within such vessels are scarce and so flow visualisation and Particle Image Velocimetry studies were undertaken to characterise the flow and measure shear levels within it.

Bioreactor Flow Visualisation

Experimental Model Configuration

A purpose-built rig has been constructed to allow flow visualisation and measurement while also producing the desired flow conditions of the bioreactor model described above. As illustrated in Figure 1, the rig consists of a polished Perspex container mounted on a rigid base with a 65mm diameter cylindrical hole drilled through its centreline to form a working section. The outer surface of the block is kept flat with square walls so that refraction effects are minimised, preventing optical distortions which may impair the image-based measurement techniques used. For similar reasons Perspex, which has a refractive index close to that of water, is used as the container material.

The swirling motion within the working section is controlled by a flat turntable rotated at constant speed using a high-resolution stepper motor. Precise mounting of the turntable and high accuracy in the rotation rate help to minimise turbulence and allow accurate control of Reynolds number. In addition, the model stand and motor bracket are screwed directly onto a precision flat steel optical table in order to reduce mechanical vibration.

Flows within cylindrical vessels driven by a rotating bottom are known to produce vortex breakdown under certain conditions. Flows are generally classified in terms of two parameters-the container height ratio (H/R) and the Reynolds number $(Re = \omega R^2/\nu)$, where H is the height of the free surface above the impeller, R is the radius of the working section, ω is the rotational velocity of the bottom disc, and ν is the kinematic viscosity.

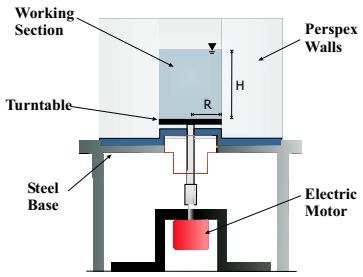

Figure 1: Test rig configuration, indicating height ratio

For the current study, experiments were conducted at $500 \leq Re \leq 3000$ and $H/R = 1.5$. It is in this range that the flow is expected to be most suitable for cell culture, being not overly turbulent whilst still providing adequate mixing. For the configuration used, with a low Froude number and a Capillary number of order 10^{-4}, free-surface deformations were restricted to the extent that they were not detected macroscopically and are thus unlikely to greatly affect the bioreactor flow conditions. The free surface is not stress-free, as minor contamination is known to induce a Marangoni stress. However, the implications of this do not seem to be severe, as results produced numerically with a slip boundary condition are qualitatively similar to our experimental results [8].

Visualisation of Vortex Breakdown Development

The flows observed within the bioreactor have a dominant azimuthal component. However it is the secondary flow pattern, which is best viewed on a vertical plane through the rig centreline, that provides much of the mixing effect. While there is high shear along the bottom and side boundary layers acting in three dimensions, the component of shear stress aligned along

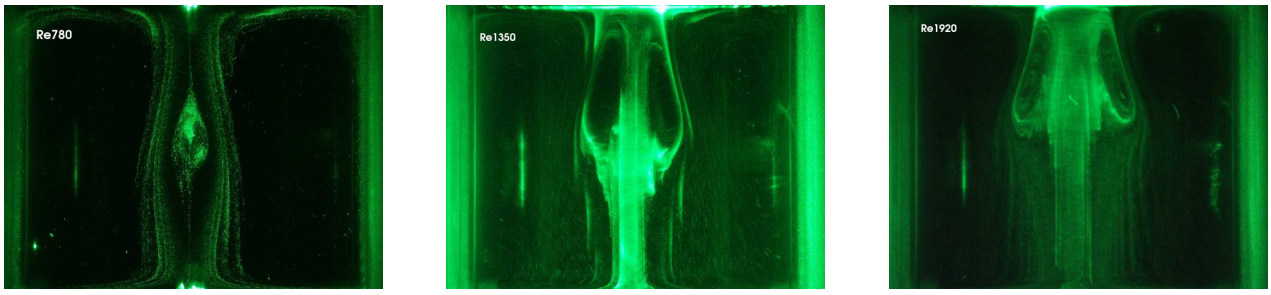

(a) (b) (c)

Figure 2: Laser particle visualisation of VB bubble development for *(a)* $Re = 780$, (b) $Re = 1350$, and *(c)* $Re = 1920$

the $x-z$ plane is a good indicator of the stresses caused by the occurance of vortex breakdown (VB).

Flow visualisation experiments were conducted using tracer particles illuminated by a high-powered laser. The particles produce distinctive streaklines as long-exposure images are captured; this can be seen in the results presented in Figure 2. The visualisation images produced were found to correspond well with Spohn et al.'s [5] observations of vortex breakdown (VB) in a cylindrical vessel with a free surface, although in the present investigation a greater number of *Re* cases were studied for a reduced H/R range.

The lowest Reynolds number at which VB was observed at this H/R was approximately 780. VB can be identified on the secondary flow plane by a separate region of recirculating flow moving in an opposing direction to the larger recirculation region. There is an stagnation point upstream of this VB bubble for cases where it is fully submerged. At higher *Re*, the bubble may be attached to the free surface, as can be seen in Figure 2, in which case the stagnation point is replaced by a stagnation ring. Once attached to the free surface, a noticeable widening of the bubble occurs as *Re* increases. At $Re \geq 2000$, an increasing flow unsteadiness was observed. Below this *Re*, the flow retains its near-axisymmetric geometry. However, as the flow takes on a more oscillatory nature, asymmetries appear to be exacerbated. These asymmetries may arise from the development of a rotating wave instability [2] or the imperfections which are inherent in any experimental rig [9].

Flow Characterisation

Flow Measurement Technique

The flow was characterised using Particle Image Velocimetry (PIV) and Stereoscopic Particle Image Velocimetry (SPIV). PIV is a well-documented technique involving the measurement of a two-dimensional velocity field by correlating the relative positions of laser-illuminated, neutrally-buoyant particles, across two images separated by a known time interval. SPIV utilises two cameras placed at a known angle to resolve all three velocity components.

For the current SPIV study, the two cameras were placed an angle of 45° from the centreline in an angular displacement configuration similar to that described by Prasad [3]. In this configuration, the x-axis of the image is stretched in relation to the y-axis, so the effective field of view is reduced by a factor of $\sqrt{2}$ in the cylinder's axial direction.

While the velocity fields measured using each technique were similar, the SPIV results are more reliable for several reasons. Firstly, for a single-camera view, the azimuthal velocity component appears as an erroneous radial velocity component. This is particularly a problem towards the central axis of the cylinder, where in-plane velocities are low, and the laser light-sheet is relatively thick compared with the path distance of a particle swirling about the central axis. Secondly, the out-of-plane velocity component adds error to in-plane velocity measurements, particularly towards the outer edges of the image. As the flow is predominantly azimuthal in this case, the ratio of the out-of-plane flow velocity to in-plane velocity is severe. This effect was eliminated to some extent in PIV experiments by using a telecentric lens.

Aside from reasons of accuracy, SPIV measurements provided a superior flow characterisation because information pertaining to the azimuthal-component of velocity is of interest to this application. Therefore the results discussed in this section are those measured using SPIV.

Secondary Flow Pattern

Spohn et al. [6] previously measured the secondary flow pattern within a cylindrical vessel with a free surface driven by a rotating disk. Their results failed to resolve all the details of the flow observed by flow visualisation. The current study, undertaken using a more precise SPIV technique, produced a velocity field which contains substantially more detail, albeit with a reduced field of view.

The flow field was measured for $H/R = 1.5$ and $500 \leq Re \leq 3000$ between horizontal positions of $0.25 \leq x/D \leq 0.75$ and axial positions of $0.56 \leq z/H \leq 0.94$. Figures 3 and 4 contain the flow field at a Reynolds number of 1200 averaged, for the sake of clarity, over 2 seconds (equivalent to approximately one third of a disk rotation). In Figure 3 streamlines illustrate the flow topology near the centre of the bioreactor. Towards the centre of the vessel ($x/D = 0.5$), the clockwise rotating recirculation region observed during flow visualisation is apparent. This distinguishing feature of the flow has seldom been captured by flow measurement. Streamlines on the right-hand side of the plot trace a portion of the counter-clockwise rotating flow region.

In Figure 4, in-plane velocity component vectors are superposed onto contours of the azimuthal velocity component. Upon detailed examination of these results and the instantaneous vector fields, it is noticeable that the VB region contains several vec-

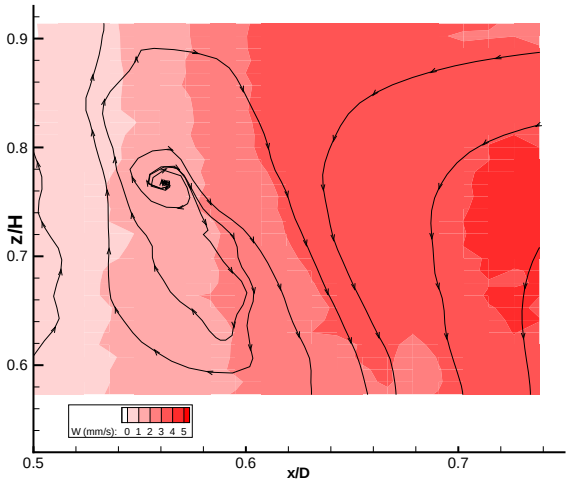

Figure 3: Flow topology in the central region of the bioreactor for $Re = 1200$. Red contours indicate the magnitude of the azimuthal velocity component. Measured streamlines indicate the flow in the diametral plane.

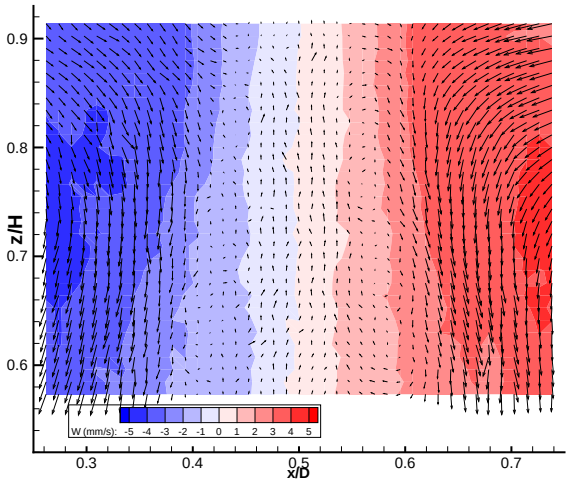

Figure 4: Measured velocity vector field in the central region of the bioreactor for $Re = 1200$. Coloured contours indicate the magnitude and direction of the azimuthal velocity component.

tors pointing away from the typical flow. While it is difficult to be certain of the reason for this, experimental noise resulting from the small displacement measurements is a possible explanation. In some cases the PIV measurements were $\ll 1$ pixel, although this could not be avoided due to difficulties in measuring flows of this nature.

In general, the velocity field shows a high degree of axisymmetry, particularly in the axial component of velocity. It is also apparent that cells within the VB region of a bioreactor will be exposed to far lower velocities than those in the standard recirculation region. The issue of whether particles can be contained within this region for long periods of time is a significant one, especially at high *Re* where instabilities and the increased opening of the downstream end of the bubble may cause cells

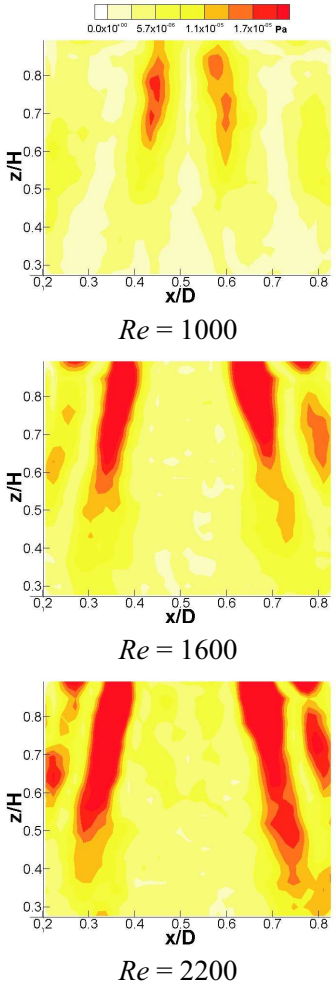

Figure 5: Time-averaged two-dimensional shear stress contours in the central region of the bioreactor for $Re = 1000, 1600, 2200$.

to escape into the high-velocity region.

Azimuthal Velocity Component

The azimuthal velocity contours plotted in Figure 4 confirm that the primary flow is axisymmetric about the central axis of the cylinder, and that the magnitude of the azimuthal velocity component is much greater than the axial and radial velocity components.

There is some limited dependency of azimuthal velocity on axial position, particular at the outer radial positions. This possibly arises from the shift in the direction of flow momentum near the free surface, or the influence of the bubble region.

Shear-Stress Fields

Shear stress is the flow characteristic of primary interest to researchers studying cell cultures. For this reason, the velocity fields measured experimentally have been used to compute shear stress contour maps for the region of the bioreactor that was investigated. If the assumption is made that time-averaged shear within the azimuthal plane is negligible, then SPIV data provides all the flow gradients required to estimate the full stress tensor, and therefore the principal stresses, at each vector loca-

tion. At the time of publication, the means of presenting these values is being developed.

The shear stress fields shown in Figure 5 are contours of time-averaged shear-stress in the vertical diametral plane ($\tau_{xz} = \mu[\frac{\partial v_x}{\partial z} + \frac{\partial v_z}{\partial x}]$, where μ is dynamic viscosity), measured using PIV. These results are useful in that they reflect the trends observed for the principle stresses in the central region of the bioreactor. While these measurements are not as accurate as the SPIV measurements towards the center of the vessel, they encompass a significantly larger field of view ($0.28 \leq z/H \leq 0.89$). The results presented have also been validated by two dimensional numerical flow simulations that produced τ_{xz} contours of similar magnitude and geometric pattern [8].

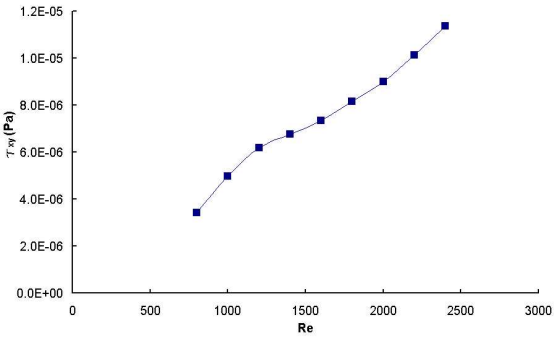

Figure 6: Mean shear levels at various *Re*

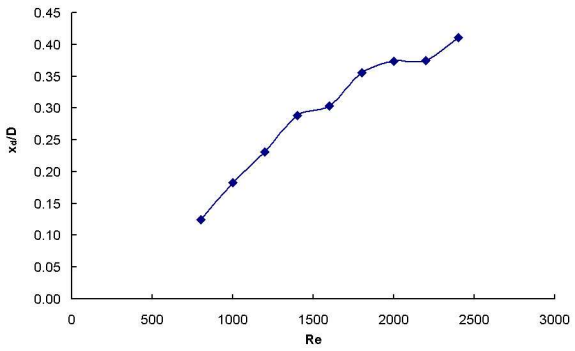

Figure 7: Horizontal distance between local shear level maxima at various *Re*

The VB bubble causes a heterogeneous stress distribution in the central region of the bioreactor. High stress bands mark the boundary of the breakdown bubble, where the high and low velocity regions border one another. In each case studied, time-averaged stress magnitudes were less in the breakdown region than in the standard recirculating flow region, although temporal fluctuations were higher in this region.

As can be expected, the mean stress levels are highly dependent on *Re*. Figure 6, in which the spatial mean τ_{xz} is plotted against *Re* provides another illustration of this. Reynolds number also controls the width of the breakdown region, and so it follows that the internal low stress region increases in volume as *Re* increases. At an axial position of $z/H = 0.6$, the horizontal distance x_d between peak shear levels increases with *Re*, although this increase tapers off at higher *Re* values, where the breakdown region tends towards its maximum width. This trend is presented in Figure 7, with x_d normalised against cylinder diameter.

All recorded levels of τ_{xz} are orders of magnitude below those typically observed for cell disruption, although use of a cell culture medium with a higher viscosity than water would directly increase these magnitudes. They also represent stresses in a conveniently located plane, and are thus only indicative of the principal stress trends measured using SPIV, rather than a quantitative measure of the maximum stresses experienced by cells. Indeed, cell geometry and orientation would also be expected to influence shear stress.

Conclusions

Laser-particle visualisation, PIV, and SPIV techniques have been employed to study how low shear swirling flows within a cylindrical bioreactor may be controlled to provide conditions suitable for cell culture applications. The flow in the vicinity of VB bubbles contained within the flow field has been found to affect conditions relevant to suspension cell culture, including mixing patterns and local shear stress. In particular, shear stress magnitudes increase rapidly as Reynolds number increase, and alter their spatial distribution as the VB region changes shape.

Acknowledgements

Funding for this research was provided by Monash University through the Monash University Research Fund and an Australian Research Council Discovery Grant (DP0452664).

References

[1] Freed, L. and Vunjak-Novakovic, G., Tissue engineering bioreactors, in *Principles of Tissue Engineering*, editors R. Lanza, R. Langer and J. Vacanti, Academic Press, San Diego, USA, 2000, 143–156.

[2] Hirsa, A., Lopez, J. and Miraghaie, R., Symmetry breaking to a rotating wave in a lid-driven cylinder with a free surface: experimental observation, *Physics of Fluids*, **14**, 2002, L29–L32.

[3] Prasad, A., Stereoscopic particle image velocimetry, *Experiments in Fluids*, **29**, 2000, 103–116.

[4] Sen, A., Kallos, M. S. and Behie, L. A., Effects of hydrodynamics on cultures of mammalian neural stem cell aggregates in suspension bioreactors, *Ind. Eng. Chem. Res.*, **40**, 2001, 5350–5357.

[5] Spohn, A., Mory, M. and Hopfinger, E. J., Observations of vortex breakdown in an open cylindrical container with a rotating bottom, *Experiments in Fluids*, **14**, 1993, 70–77.

[6] Spohn, A., Mory, M. and Hopfinger, E. J., Experiments on vortex breakdown in a confined flow generated by a rotating disk, *Journal of Fluid Mechanics*, **370**, 1998, 73–99.

[7] Sucosky, P., Osorio, D. F., Brown, J. B. and Neitzel, G. P., Fluid mechanics of a spinner-flask bioreactor, *Biotechnology and Bioengineering*, **85**, 2004, 34–46.

[8] Tan, B. T., Personal correspondence.

[9] Thompson, M. C. and Hourigan, K., The sensitivity of steady vortex breakdown bubbles in confined cylinder flows to rotating lid misalignment, *Journal of Fluid Mechanics*, **496**, 2003, 129–138.